



HAL
open science

Effect of the incident power on permittivity, losses and tunability of BaSrTiO₃ thin films in the microwave frequency range

Kevin Nadaud, Caroline Borderon, Raphaël Renoud, Areski Ghalem, Aurelian Crunteanu, Laure Huitema, Frédéric Dumas-Bouchiat, Pascal Marchet, Corinne Champeaux, Hartmut W Gundel

► To cite this version:

Kevin Nadaud, Caroline Borderon, Raphaël Renoud, Areski Ghalem, Aurelian Crunteanu, et al.. Effect of the incident power on permittivity, losses and tunability of BaSrTiO₃ thin films in the microwave frequency range. *Applied Physics Letters*, 2017, 110 (21), pp.212902. 10.1063/1.4984089 . hal-01525619

HAL Id: hal-01525619

<https://hal.science/hal-01525619v1>

Submitted on 22 May 2017

HAL is a multi-disciplinary open access archive for the deposit and dissemination of scientific research documents, whether they are published or not. The documents may come from teaching and research institutions in France or abroad, or from public or private research centers.

L'archive ouverte pluridisciplinaire **HAL**, est destinée au dépôt et à la diffusion de documents scientifiques de niveau recherche, publiés ou non, émanant des établissements d'enseignement et de recherche français ou étrangers, des laboratoires publics ou privés.

Effect of the incident power on permittivity, losses and tunability of BaSrTiO₃ thin films in the microwave frequency range

Kevin Nadaud,^{1, a)} Caroline Borderon,^{2, b)} Raphaël Renoud,² Areski Ghalem,³ Aurelian Crunteanu,³ Laure Huitema,³ Frédéric Dumas-Bouchiat,⁴ Pascal Marchet,⁴ Corinne Champeaux,⁴ and Hartmut W. Gundel²

¹⁾GREMAN, UMR CNRS 7347, Université François Rabelais de Tours, 16 rue Pierre et Marie Curie, 37071 Tours Cedex 2, France

²⁾IETR, UMR CNRS 6164, Université de Nantes, 44322 Nantes, France

³⁾XLIM, UMR CNRS 7252, Université de Limoges, 123 avenue Albert Thomas, 87060 Limoges, France

⁴⁾Univ. Limoges, CNRS, SPCTS, UMR 7315, 12 rue Atlantis, F-87068 Limoges, France.

Domain wall motions in ferroelectrics participate to the material's complex permittivity and are responsible for their sensitivity of the dielectric properties to the driving electric field and thus to the incident power at microwave frequencies. In the present study, the dependence of the permittivity, the dielectric losses and the tunability of Ba_{2/3}Sr_{1/3}TiO₃ (BST) thin films on the incident power and on the bias fields is examined at a frequency of 500 MHz. While, the domain wall motion participates only slightly to the permittivity (< 5%), it strongly influences the losses due to its very dissipative behavior. As a consequence, the Figure of Merit (*FoM*, ratio between tunability and dielectric losses) of the material depends on the applied microwave power. In the present study, a decrease of the *FoM* from 29 to 21 is observed for an incident power varying from -20 dBm to 5 dBm. When characterizing ferroelectric materials, the incident power has to be considered; moreover, domain wall motion effects should be limited in order to achieve a high *FoM* and less power sensitivity.

Keywords: Ferroelectrics, domain walls, hyperbolic law, microwave frequency, tunability, FoM

^{a)}Electronic mail: kevin.nadaud@univ-tours.fr

^{b)}Electronic mail: caroline.borderon@univ-nantes.fr

Ferroelectric tunable materials are very promising for the realization of reconfigurable microwave devices. The main advantage is small power consumption due to a low leakage current¹⁻³. For this kind of application, it is necessary to have both a high tunability of the relative permittivity ε'_r and low dielectric losses $\tan \delta$, which is not straightforward as both phenomena are linked. In order to represent the compromise between a high tunability and low losses, the *FoM* is usually defined as:⁴

$$FoM = \frac{n_r(\%)}{\tan \delta \times 100}, \quad (1)$$

where $\tan \delta$ is the dielectric losses at 0 V and $n_r(\%)$ corresponds to the relative tunability given in percent:

$$n_r(\%) = \frac{\varepsilon'_r(0) - \varepsilon'_r(E_{DC})}{\varepsilon'_r(0)} \times 100, \quad (2)$$

with $\varepsilon'_r(0)$ and $\varepsilon'_r(E_{DC})$ the permittivity without and under the bias electric field E_{DC} , respectively. For the calculation of the *FoM*, $\tan \delta$ is multiplied by 100 in order to convert it into percent and to have a homogeneity with the tunability. The higher is the *FoM*, the more the material properties are suitable for microwave applications. As ferroelectric materials are non-linear materials, the *FoM* depends not only on the frequency but also on the power of the incident wave, which modifies the dielectric properties at low driving fields due to domain wall motion⁵ and at high driving fields due to switching^{6,7}. Domain wall motion particularly creates a sensitivity of the permittivity to the driving field⁸⁻¹² and this latter also influences the dielectric losses which conditions the *FoM*¹³. Contrary to the frequency, the incident power is often not indicated when reporting the *FoM* of a ferroelectric material.

In the present paper, the influence of the incident power on the dielectric properties of a ferroelectric thin film in the microwave range is studied and more especially when a bias field is applied. We focus on a moderate power (corresponding to a low driving field E_{AC}) in order to only obtain domain wall motion (Rayleigh region) but no variation of the domain wall density. The study is done on (100) epitaxial $\text{Ba}_{2/3}\text{Sr}_{1/3}\text{TiO}_3$ (BST) thin films deposited by pulsed laser deposition on a (100)-oriented MgO/Ir substrate. More details on the process and the structural characterization are reported elsewhere^{5,14}. The film has a thickness of 0.45 μm and it consists of highly oriented columnar grains of approximately 0.1 μm in width.

The dielectric characterizations are performed using a metal-insulator-metal (MIM) parallel plate capacitor geometry (Fig. 1). The advantage is the possibility to perform measurements at low and high frequencies and the easy permittivity calculation using the parallel

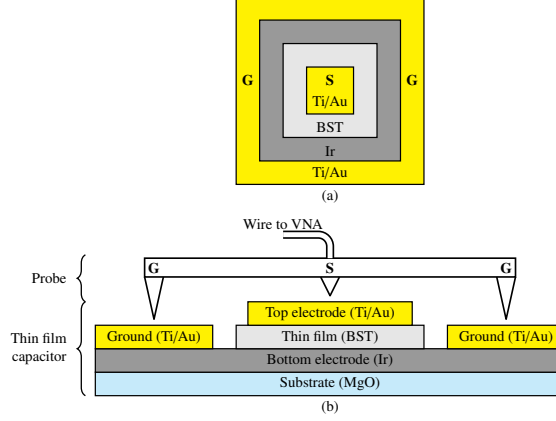


Figure 1. Topology of the considered MIM ferroelectric capacitor. Top view (a) and stack-up (b).

plate formula. The bottom electrode consists of an iridium layer (100 nm) while the square top electrode ($30 \times 30 \mu\text{m}^2$) is made of gold/titanium (200 nm/10 nm). The capacitor is measured using a Cascade ground-signal-ground (GSG) probe of $125 \mu\text{m}$ pitch and a vector network analyzer (VNA, Rohde & Schwarz ZVA24) at a frequency of 500 MHz and at room temperature (20°C). A bias-tee allows us to apply the DC voltage to the capacitor. The impedance of the capacitor is determined using the reflected S -parameter Γ_C :

$$Z_C = Z_0 \frac{1 + \Gamma_C}{1 - \Gamma_C}, \quad (3)$$

where Z_0 is the reference impedance (50Ω). The capacitance C and $\tan \delta$ are determined using following formula:¹⁵

$$C = \text{Re} \left[\frac{1}{j\omega Z_C} \right], \quad (4)$$

$$\tan \delta = -\frac{\text{Re}[Z_C]}{\text{Im}[Z_C]}, \quad (5)$$

with ω the angular frequency.

The incident power has been varied from -20 dBm to 5 dBm (corresponding to $E_{AC} < 17$ kV/cm) and the bias voltage from 0 V to 10 V with voltage steps of 0.5 V. This corresponds to a maximum bias field of 222 kV/cm with a step of 11 kV/cm for the 450 nm thick film. In addition to the reflection calibration, a power calibration has been performed and the indicated power thus corresponds to the real power incident on the ferroelectric capacitor.

The extracted relative permittivity and the dielectric losses as a function of the bias field for two incident power values are shown in Fig. 2. As the $\text{Ba}_{2/3}\text{Sr}_{1/3}\text{TiO}_3$ corresponds to a

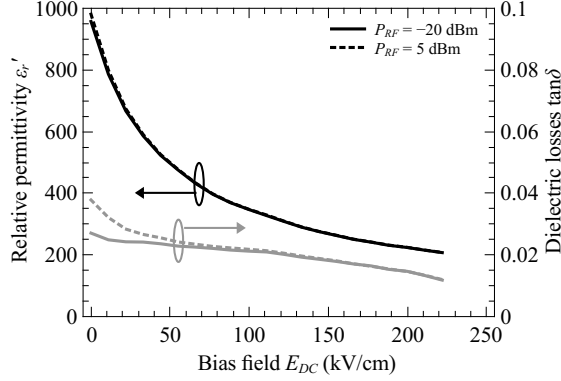


Figure 2. Relative permittivity and dielectric losses as a function of the bias field for two incident powers.

composition in a paraelectric phase¹⁶, the two characteristics do not present a coercive field and decrease with increasing bias electric field. At zero bias field, the effect of the incident power on the permittivity is very small. Only a slight increase from 957 to 980 can be observed, corresponding to a variation of less than 2.5%. This increase is due to the domain wall pinning/unpinning contribution to the permittivity which is enhanced when the driving field (or incident power) increases^{5,8,9}. This clearly indicates the presence and the movement of domain walls even if the BST is considered to be in the paraelectric phase¹⁷. Above 50 kV/cm, no influence on the relative permittivity is seen as domain coalescence appears¹⁸, which reduces the domain density. As the domain wall pinning/unpinning contribution depends on the number of domain walls¹⁹, its contribution to the permittivity is also reduced and the incident power has less impact. As a consequence, the ferroelectric tunability at 222 kV/cm is rather independent from the incident power. The small variation observed (from 78.3% at -20 dBm to 78.8% at 5 dBm) is due to the slight difference in permittivity at zero bias.

The increase of the dielectric losses at low bias field as a function of the incident power (from 0.027 to 0.038, corresponding to an increase of 40%) is more apparent than the variation of the permittivity. This is due to the fact that domain wall motion is a very dissipative phenomena^{5,13,20}. When the bias field increases, the sensitivity to the incident power decreases quickly. At 50 kV/cm, the losses differ only about 5% and beyond 100 kV/cm, there is almost no discernable difference. As a consequence of the sensitivity of the dielectrics properties, the FoM of the material also depends on the incident power and varies from 29

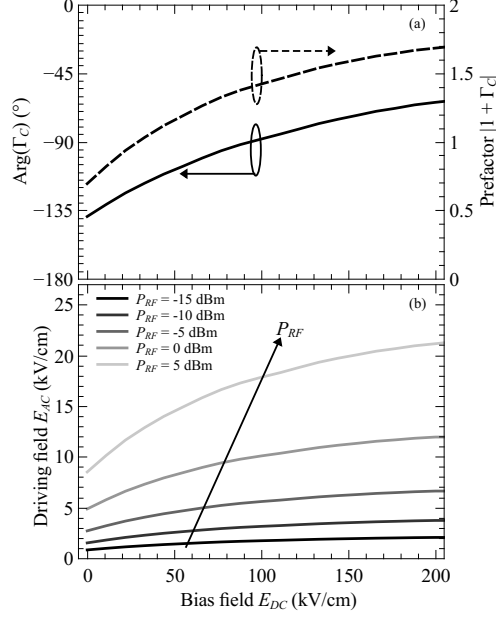


Figure 3. Reflection coefficient (8), prefactor $|1 + \Gamma_C|$ (a) and driving field for different incident power (b) as a function of the bias field.

to 21 for applied powers of -20 dBm and 5 dBm respectively. FoM is largely influenced by the incident power at microwave frequencies, similar to findings in Ref. 13.

In order to study the different contributions of domain wall motion to the FoM , the Rayleigh law can be used to describe the variation of the permittivity as a function of the driving field E_{AC} ⁸. In the present case, however, the hyperbolic law has been preferred since it describes also the permittivity below the threshold field of domain wall pinning⁹. At fields higher than E_{th} , the two laws are similar. Thus, the permittivity is described by:

$$\varepsilon_r = \varepsilon_{rl} + \sqrt{\varepsilon_{r-rev}^2 + (\alpha_r E_{AC})^2}, \quad (6)$$

where ε_{rl} corresponds to the lattice contribution, ε_{r-rev} to the domain wall vibration and α_r to pinning/unpinning of the domain walls. These two latter contributions are only present in ferroelectric materials where the polarization is organized into domains and can reveal a residual ferroelectricity for BST thin films in the paraelectric state¹⁷. The hyperbolic law can be applied if the driving field E_{AC} is sufficiently low compared to the material's coercive field in order to not provoke a change of the global domain configuration (Rayleigh region)¹⁹.

When using a VNA for the measurement, only the incident power P_{RF} can be set and a

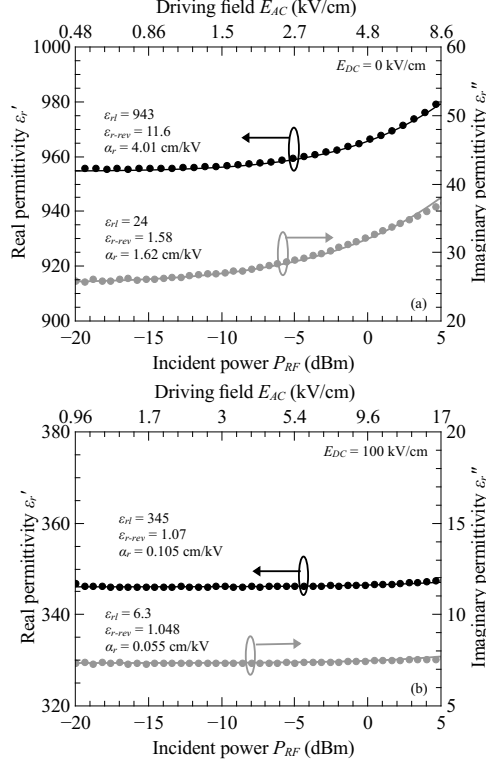


Figure 4. Real and imaginary parts of the permittivity as a function of the incident power without bias field (a) and at 100 kV/cm (b). The hyperbolic fits allow retrieving the different contributions using (6) and the corresponding driving fields are calculated using (7).

conversion into the actual driving field E_{AC} ⁵ is necessary:

$$E_{AC} = \frac{V_{AC}}{t_{BST}} = |1 + \Gamma_C| \frac{\sqrt{2Z_0 P_{RF}}}{t_{BST}}, \quad (7)$$

with t_{BST} the thickness of the thin film and Γ_C the reflection coefficient of the load which can be written as:

$$\Gamma_C = \frac{1 - j\omega Z_0 C(P_{RF}, E_{DC})}{1 + j\omega Z_0 C(P_{RF}, E_{DC})}, \quad (8)$$

where $C(P_{RF}, E_{DC})$ is the capacitance of the tunable material. For a given ω , the reflection coefficient depends on the capacitance $C(P_{RF}, E_{DC})$ which itself depends on the incident RF power P_{RF} and bias field E_{DC} . In the present case, the capacitance varies from 17 pF at zero bias field to 3.6 pF for a bias field of 222 kV/cm. As a consequence, the argument of the reflection coefficient changes from -135° to -60° and the prefactor $|1 + \Gamma_C|$ thus varies from 0.69 to 1.7 (Fig. 3a).

In order to discern the different contributions, the real and imaginary parts of the per-

mittivity have been measured as a function of the incident power and bias field. Fig. 4 shows the values obtained without bias field and for a field of 100 kV/cm. The equivalent driving field is different in both cases since the value of the reflection coefficient changes when the capacitance is tuned by the DC field. In the case of the measurement without bias (Fig. 4a), the increase of the real and imaginary parts as a function of the driving field is readily apparent (about 23 and 11 unities respectively). The evolution of the real and imaginary parts of the permittivity with the incident power is very small (less than 1 unity), for the measurement at 100 kV/cm bias field (Fig. 4b), even though the equivalent driving field is larger. This small change is due to almost negligible domain wall pinning/unpinning at high DC fields (represented by a lower value of the α_r parameter). This clearly indicates that the bias field changes the contribution of the domain wall pinning/unpinning to the complex permittivity in the microwave region, similar to what has been shown at lower frequency^{13,21}.

Fitting the real and imaginary parts of the permittivity as a function of the incident power with the hyperbolic law (6) allows us to obtain the different contributions to the permittivity. In order to correctly fit the data, the actual driving field associated with the incident power has to be computed for each bias field since the prefactor $|1 + \Gamma_C|$ varies. The different contributions to the permittivity are shown in Fig. 5. In order to assess its influence on the material's properties, the generalized expression of the Figure of Merit written as FoM_ε ¹³ shall be used. This value is based on the generalized tunability $n_{r-\varepsilon}$ and the dissipation factor $m_\varepsilon = \varepsilon''/\varepsilon'$ where ε may be respectively the contribution ε_{rl} , ε_{r-rev} or α_r .

The lattice contribution depends on the bias field (Fig. 5a), similar to what is observed for the overall permittivity since it represents the main part of the real permittivity (see Table I). The relative tunability, $n_{r-\varepsilon_{rl}}$, of this contribution is close to the total tunability but the dissipation factor of the lattice, $m_{\varepsilon_{rl}}$, is smaller than the overall value of the dissipation factor. This indicates that other contributions participate to the overall losses. Even though the imaginary part of the lattice contribution represents the most important part of the losses, the relative weight is smaller especially at a power of 5 dBm. Therefore, the $FoM_{\varepsilon_{rl}}$ of the lattice contribution is higher than the FoM of the overall permittivity.

A rapid decrease of the domain wall vibration contribution with increasing bias field is shown in Fig. 5b. When a bias field is applied¹⁸, domain coalescence causes a reduction of

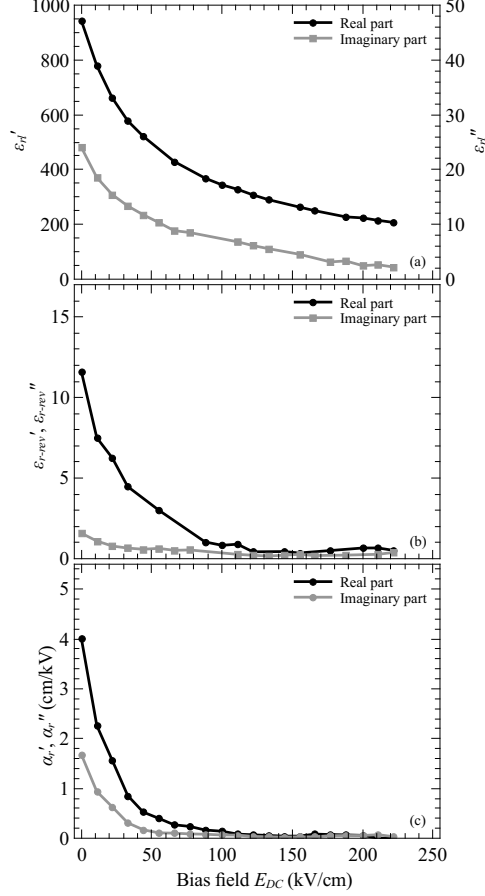


Figure 5. Real and imaginary parts of the lattice (a), domain wall vibration (b) and domain wall pinning/unpinning (c) contributions to the permittivity as a function of the bias field.

the domain wall density. This decrease is consistent with the observation that the vibration contribution is proportional to the domain wall density¹⁹. At high bias fields, the vibration contribution approaches zero indicating the domain wall density is very small. Therefore, the contribution of the domain wall vibration to the overall permittivity and losses is low (Table I). The tunability $n_{\epsilon_{r-rew}}$ is high, however, the large dissipation factor confirms that the domain wall vibration is more lossy than the lattice contribution^{5,13,22}. As a consequence, the $FoM_{\epsilon_{r-rew}}$ for this contribution is relatively low (around 6.1).

The evolution of the pinning/unpinning coefficient as a function of the bias field is shown in Fig. 5c. As with the vibration contribution, the real and imaginary parts of the coefficient decrease with increasing bias field. Domain wall pinning/unpinning also depends on the domain wall density¹⁹, which explains the observed behavior. At high bias fields, the contribution tends to zero, indicating that domain wall pinning/unpinning no longer con-

Table I. Weight of the different contributions into the overall permittivity and losses for an incident power of -20 dBm and 5 dBm without bias field. Tunability and FoM at 222 kV/cm.

Contribution	P_{RF}	Permittivity Weight	Losses Weight	Loss factor	Tunability	FoM
Lattice	-20 dBm	98.6 %	92.8 %	0.025	78 %	31
	5 dBm	96.2 %	64.8 %			
Vibration	-20 dBm	1.2 %	4.7 %	0.15	91 %	6.1
	5 dBm	1 %	3.5 %			
Pinning/ unpinning	-20 dBm	0.2 %	2.4 %	0.42	99 %	2.4
	5 dBm	2.8 %	31.7 %			
Total	-20 dBm			0.027	78.3 %	29
	5 dBm			0.038	78.8 %	21

tributes to the permittivity. The contribution to the overall permittivity and losses is also low according to the domain wall density in the material. The tunability of this contribution is huge but the observed dissipation factor m_{α_r} is also very high (Table I). Pinning/unpinning thus has been found to be 2.7 times more dissipative than domain vibration and 16 times more dissipative than the lattice and the associated FoM_{α_r} is very small (2.4).

Finally, at microwave frequencies, domain wall motion (vibration and pinning/unpinning) still contributes to the material's dielectric properties. Despite being highly tunable, the highly dissipative character of domain wall motion results in a considerably smaller FoM compared to the lattice contribution which dominates the permittivity value and has low losses. The weight of the respective contribution in the overall permittivity and losses for an incident power of -20 dBm and 5 dBm without bias along with the tunability and the FoM at 222 kV/cm are summarized in Table I. While intrinsic tunability $n_{r-\epsilon}$ and the dissipation factor m_ϵ are not affected by the incident power, their weight into the overall permittivity and losses does depend on incident power. Further, the domain pinning/unpinning contribution strongly increases with incident power. As a consequence, the overall FoM of the ferroelectric thin film decreases.

The overall tunability of the ferroelectric thin film and the corresponding FoM at 500 MHz

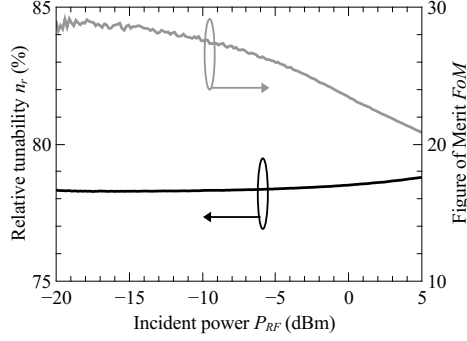


Figure 6. Relative tunability and Figure of Merit as a function of the incident power for DC bias field of 222 kV/cm.

are shown in Fig. 6 as a function of the incident power. The slight increase of the tunability ($\approx 0.5\%$) comes from the enhanced contribution of domain wall pinning/unpinning to the material's permittivity at higher incident power. The drop of the FoM value of almost 30% for a power varying from -20 dBm to 5 dBm is much more pronounced. This drop is due to the influence of the very dissipative behavior of the pinning/unpinning (see also Table I). This trend clearly indicates the effect of the RF power on the dielectric properties of tunable ferroelectric thin films and confirms that the low frequency effects observed in Ref. 13 apply at microwave frequencies.

In this paper, the effect of the incident power on the permittivity, losses and tunability has been shown for a BST thin film. Determination of the different contributions to the complex dielectric permittivity by the hyperbolic law shows that the driving field influences the dielectric properties even at microwave frequencies. This influence is due to domain wall motion which is still present at high frequencies. When increasing the incident power, the very dissipative pinning/unpinning phenomenon gets an enhanced influence on the overall dielectric losses and thus on the Figure of Merit of the material. Therefore, the incident power should be taken into account when characterizing a tunable material. Domain wall pinning/unpinning should be limited in order to obtain a large FoM .

The authors gracefully acknowledge L. Trupina and L. Nedelcu from the National Institute of Materials Physics (Romania) for the iridium bottom electrode deposition.

REFERENCES

- ¹K. Nadaud, R. Gillard, E. Fourn, H. Gundel, and C. Borderon, in *Loughborough Antennas and Propagation Conference* (2014) pp. 214–217.
- ²J. Hai, M. Patterson, D. Brown, Z. Chenhao, P. KuanChang, G. Subramanyam, D. Kuhl, K. Leedy, and C. Cerny, *IEEE Transactions on Antennas and Propagation* **60**, 3111 (2012).
- ³A. Ghalem, F. Ponchel, D. Remiens, and T. Lasri, in *Proc. IEEE Int. Symp. Applicat. Ferroelectrics* (2013) pp. 252–256.
- ⁴D. Dimos, M. Raymond, R. Schwartz, H. Al-Shareef, and C. Mueller, **1**, 145 (1997).
- ⁵K. Nadaud, C. Borderon, R. Renoud, A. Ghalem, A. Crunteanu, L. Huitema, F. Dumas-Bouchiat, P. Marchet, C. Champeaux, and H. W. Gundel, *Applied Physics Letters* **109**, 262902 (2016).
- ⁶P. Rundqvist, A. Vorobiev, E. Kollberg, and S. Gevorgian, *Journal of Applied Physics* **100**, 1 (2006).
- ⁷Y.-K. Yoon, D. Kim, M. G. Allen, J. S. Kenney, and A. T. Hunt, *IEEE Transactions on Microwave Theory and Techniques* **51**, 2568 (2003).
- ⁸D. V. Taylor and D. Damjanovic, *Journal of Applied Physics* **82**, 1973 (1997).
- ⁹C. Borderon, R. Renoud, M. Ragheb, and H. W. Gundel, *Applied Physics Letters* **98**, 112903 (2011).
- ¹⁰D. Bharadwaja, S. S. N. and Damjanovic and N. Setter, *Ferroelectrics* **303**, 59 (2004).
- ¹¹W. Zhu, I. Fujii, W. Ren, and S. Trolier-McKinstry, *Journal of Applied Physics* **109**, 064105 (2011).
- ¹²N. Gharb and S. Trolier-McKinstry, *Journal of Applied Physics* **97**, 064106 (2005).
- ¹³K. Nadaud, C. Borderon, R. Renoud, and H. W. Gundel, *Journal of Applied Physics* **119**, 114101 (2016).
- ¹⁴A. Ghalem, M. Rammal, L. Huitema, A. Crunteanu, V. Madrangeas, P. Dutheil, F. Dumas-Bouchiat, P. Marchet, C. Champeaux, L. Trupina, L. Nedelcu, and M. G. Banciu, *IEEE Microwave and Wireless Components Letters* **26**, 504 (2016).
- ¹⁵Z. Ma, A. J. Becker, P. Polakos, H. Huggins, J. Pastalan, H. Wu, K. Watts, Y. H. Wong, and P. Mankiewich, *IEEE Transactions on Electronics Devices* **45**, 1811 (1998).
- ¹⁶V. V. Lemanov, E. P. Smirnova, P. P. Syrnikov, and E. A. Tarakanov, *Phys. Rev. B* **54**,

- 3151 (1996).
- ¹⁷L. M. Garten, P. Lam, D. Harris, J.-P. Maria, and S. Trolier-McKinstry, *Journal of Applied Physics* **116**, 044104 (2014).
- ¹⁸D. Damjanovic, *Reports on Progress in Physics* **61**, 1267 (1998).
- ¹⁹O. Boser, *Journal of Applied Physics* **62**, 1344 (1987).
- ²⁰J. E. García, R. Pérez, and A. Albareda, *Journal of Physics: Condensed Matter* **17**, 7143 (2005).
- ²¹N. Bassiri-Gharb, *Dielectric and Piezoelectric Nonlinearities in Oriented Pb(Yb_(1/2)Nb_(1/2))O₃ – PbTiO₃ Thin Films*, Ph.D. thesis, Department of Materials Science and Engineering, Pennsylvania State University, University Park, Pennsylvania (2005).
- ²²K. Nadaud, C. Borderon, R. Renoud, and H. W. Gundel, *Journal of Applied Physics* **117**, 084104 (2015).